International Journal of Automotive Technology, Vol. 5, No. 4, pp. 297–302 (2004)

1229-9138/2004/018-08

LOW CYCLE THERMAL FATIGUE OF THE ENGINE EXHAUST MANIFOLD

B. L. CHOI*, H. CHANG and K. H. PARK

Hyundai Motor Company, 772-1 Jangduk-Dong, Whasung-Si, Gyeonggi 445-706, Korea

(Received 19 April 2003; Revised 4 March 2004)

ABSTRACT–This paper presents the low cycle thermal fatigue of the engine exhaust manifold subject to thermo-mechanical cyclic loading. As a failure of the exhaust manifold is mainly caused by geometric constraints of the less expanded inlet flange and cylinder head, the analysis is based on the exhaust system model with three-dimensional temperature distribution and temperature dependent material properties. The result show that large compressive plastic deformations are generated at an elevated temperature of the exhaust manifold and tensile stresses are remained in several critical zones at a cold condition. From the repetition of these thermal shock cycles, maximum plastic strain range (0.454%) could be estimated by the stabilized stress-strain hysteresis loops. It is used to predict the low cycle thermal fatigue life of the exhaust manifold for the thermal shock test.

KEY WORDS : Exhaust manifold, Thermal shock test, FEM, Plastic strain range, Thermal fatigue life

1. INTRODUCTION

Exhaust manifold is generally subjected to many repeated run-stop cyclic loadings (thermal shock) in the field. It undergoes the followings in a typical thermal shock condition; at run (or, hot) condition, large compressive plastic deformations are generated, and at stop (or, cold) condition, tensile stresses are remained in highly deformed critical zones such as runner junctions (Lederer *et al.*, 2000). These phenomena originate from that thermal expansions of the runners are restricted by inlet flange clamped to the cylinder head, because the former is less stiff than the latter and, the temperature of the inlet flange is lower than that of the runners. Therefore, we can conclude that thermal fatigue cracks in the exhaust manifold are mainly generated due to the difference of the stiffness and temperature between cylinder head and runners.

This study presents more reliable analysis results for the low cycle fatigue of the exhaust manifold due to the typical thermal shock endurance test, shortly simulating the repeated engine start-up and shutdown in the field. In thermal stress analysis, the governing equation is used with the elasto-plastic thermal constitutive relationship. And, the analysis also includes a heat transfer analysis to obtain 3-D temperature distribution for the hot condition in the thermal shock test. Later, the results of the stress analysis will be used for the life prediction process.

A number of bench tests on the exhaust manifold were also carried out to justify the validity of the analysis procedures. The comparison of the results between analysis and bench test shows a good agreement in both temperature distribution and crack locations. Additionally, creep strains may have occurred at an elevated temperature of the thermal shock mode. But, their effect on fatigue life is relatively small because they remain in a compressive strain during short times. Thus, creep strains are excluded in this analysis.

Therefore, in our experience, it is concluded that the fatigue failure of the exhaust manifold be dominated mainly by plastic strain range ($\Delta\varepsilon_P$) during thermal shock cycles (Watanabe *et al.*, 1999).

2. ANALYSIS MODEL

2.1. Analysis Procedure

The process of the thermal analysis and life prediction for the exhaust manifold is schematically shown in Figure 1 (Noguchi *et al.*, 1985). The analysis procedures are summarized as followings :

(1) Construction of the finite element model for the hot end exhaust system with a part of cylinder head.
(2) The operating conditions (flow rate, exhaust gas temperature etc.) are calculated by using the engine cycle simulation. Next, temperature distributions at each time during the thermal shock loading are

**Corresponding author.* e-mail: a1cbl@hyundai-motor.com

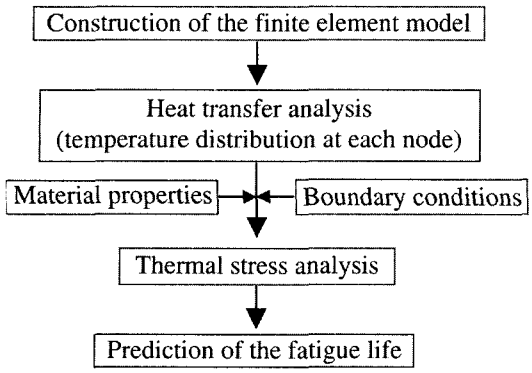

Figure 1. Analysis procedure of the exhaust manifold.

determined by Conjugate Heat Transfer (CHT) analysis.

(3) The 3-D temperature data at each time are used to simulate the thermal elasto-plastic stress analysis, which considers temperature dependent material properties but ignores creep effects.

(4) Prediction of the thermal fatigue life.

2.2. Heat Transfer Analysis (CHT Analysis)

The objective of the heat transfer analysis is to calculate the 3-D temperature distribution of the exhaust system. The results will be used as input data for the thermal stress analysis. The governing equation of conjugate heat transfer (CHT) can be expressed in terms of mass, momentum, and energy conservation laws. We also assume that the fluid field is steady state, incompressible, and turbulent model. So, the standard k-ε model is used by STAR-CD software. The input includes a mass flow rate per individual port and gas temperature of 830°C calculated by engine operating conditions and engine cycle simulation program.

In order to obtain mass flow rate, the corresponding equations and the engine specifications are as follows.

$$\dot{m} = \dot{m}_{air} + \dot{m}_{fuel} \quad (1)$$

$$\dot{m}_{fuel} = \mathrm{BSFC} \times \mathrm{P}/60 \quad (2)$$

$$\dot{m}_{air} = \dot{m}_{fuel} \times A/F \quad (3)$$

Table 1. Convection type boundary condition.

Location		T (°C)	R (m^2T/W)	h (W/m^2T)
Inlet flange	Head side	85 (coolant)	0.004	250
	Air side	139.5 (ambient)	0.004	250
Runner		139.5 (ambient)	0.070	15
Outlet flange	Air side	139.5 (ambient)	0.050	20
	CCC side	Insulated		

R (thermal resistance)=1/h (heat transfer coefficient)

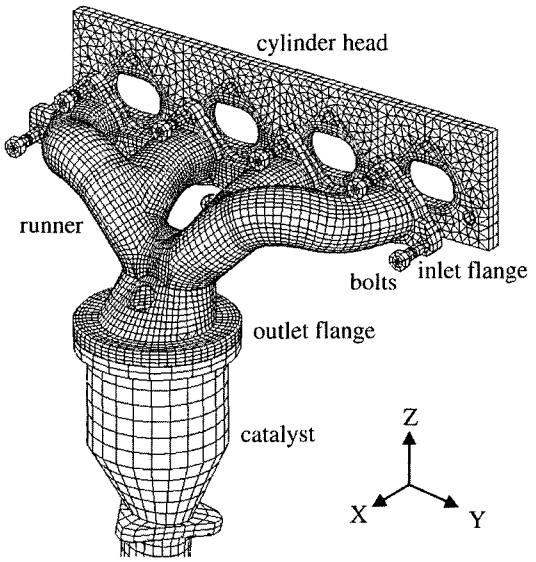

Figure 2. Construction of the finite element model.

- BSFC : 268 (g/PS·h) - Power : 137 (PS)
- A/F ratio (12 : 1) - Exhaust gas : 830°C

The boundary conditions of the fluid and solid are used as the convective type presented in Table 1.

2.3. Finite Element Model

Figure 2 shows a finite element model for the thermal stress analysis. The exhaust hot end model is composed of simple cylinder head, bolts, exhaust manifold, engine mounting bracket, and downstream pipe. As shown in figure, the manifold inlet is attached to the cylinder head, and the downstream end of the manifold assembly is attached to the engine block by the bracket. We constructed the main exhaust manifold with two layered brick element to represent the effects of the temperature difference between the inside and outside surface. And, cylinder head and catalyst are modeled with tetrahedron, shell, and rigid elements.

2.3.1. Load conditions

Generally, the exhaust manifold is fastened to the cylinder head with several bolts. So, the bolt model is used to give the pretension load on the manifold.

Next, thermal cyclic loading is applied as 3-D temperature distribution to the finite element model. It is composed of two steps; heat up and cool down. During the heat up process, the entire model except for the cylinder head is heated from room temperature to the maximum temperature distribution obtained from the CHT analysis. And, during the cool down process, the assembly model goes back to the room temperature in a steady state condition. Figure 3 shows the load steps with prescribed load history of one cycle. These are repeated

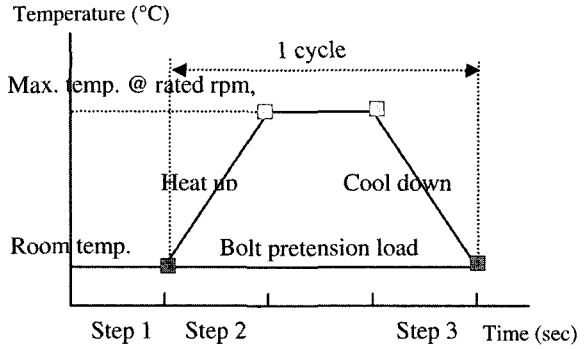

Figure 3. Load step during thermal shock test.

for several cycles until stabilized stress-strain curves are obtained.

2.3.2. Boundary condition

As shown in figure 2, the bottom surface of the cylinder head is normally restrained so that there is no movement perpendicular to the surface. And, at any point of the bottom surface of the cylinder head, the rigid body motion is also restrained in vertical and horizontal directions. And, small contact conditions are defined between the inlet flange and cylinder head and also between bolt heads and inlet flange. The friction coefficients between all contact surfaces are set to 0.2.

2.3.3. Material properties

The temperature dependent nonlinear material properties should be considered to represent the real material behavior. This is very important in the thermal analysis of the exhaust manifold, because the temperature changes greatly along the exhaust system.

Figure 4 shows stress-strain relationship of the cast iron (namely, FCD50-HS) for the exhaust manifold. Where, the plastic material curves are based on the uniaxial tension test at each temperature. As can be seen in figure, Youngs modulus and yield strength decrease

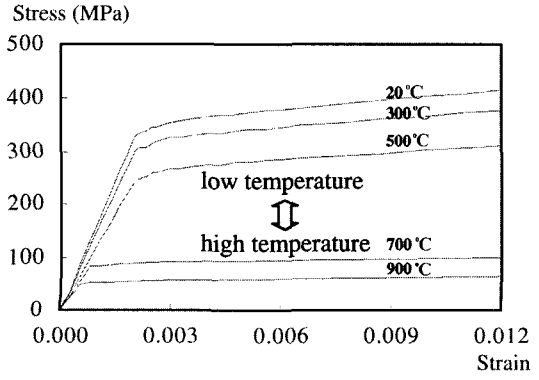

Figure 4. Stress-strain curves of cast iron (FCD_50HS).

Table 2. Material properties at room temperature.

Part	FCD-50HS	Steel	Aluminum
E (GPa)	160	205	69
ν	0.29	0.30	0.33
α (1/K) (10^{-6})	12.2	11.5	21.4

more rapidly nearby 500°C.

Table 2 shows the elastic material properties at room temperature. Where, aluminum and steel properties are used for cylinder head and bolts. Later, it is necessary to conduct extensive tests to obtain the material data for high temperature fatigue performances.

3. ANALYSIS RESULTS

In order to progress the elasto-plastic thermal stress and fatigue analysis, it is necessary to consider the temperature distribution, mechanical constraints, and temperature dependent material properties as described in previous section (Kawano *et al.*, 1991).

3.1. Thermal Shock Endurance Test

To verify the structural durability under thermal shock loads, a standard durability test is typically performed in the development stage. Figure 5 is the simple thermal

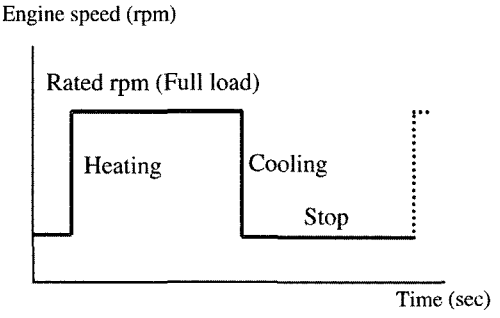

Figure 5. Thermal shock condition.

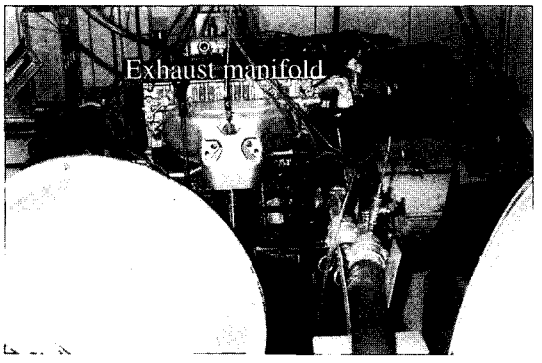

Figure 6. Test apparatus of thermal shock.

shock mode to simulate the thermal load cycle consisted by the heating and cooling process. One cycle consists of idling, full load at the rated speed that gives maximum power, and cooling process to the ambient temperature. Figure 6 shows the test equipment to simulate the thermal shock. The test and operating conditions are as follows.

(a) Test condition (blow fan on)
- Rated rpm, WOT (Wide Open Throttle)
- Engine stop

(b) Operating condition
- W/T (water temp.) : 95±3°C–30°C
- O/T (oil temp.) : 145°C

3.2. Temperature Distribution

The temperature field was calculated in a steady state condition at rated rpm and WOT (Wide Open Throttle) state. Figure 7 shows general temperature history of any locations of the exhaust manifold during thermal shock load. Where, point O is the start point at room temperature, and heating up along O-B, and finally decreases from B to C during cool down process.

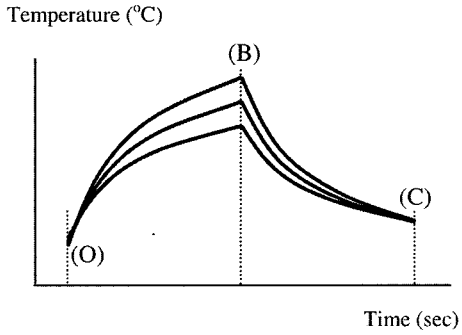

Figure 7. Temperature profile during thermal shock.

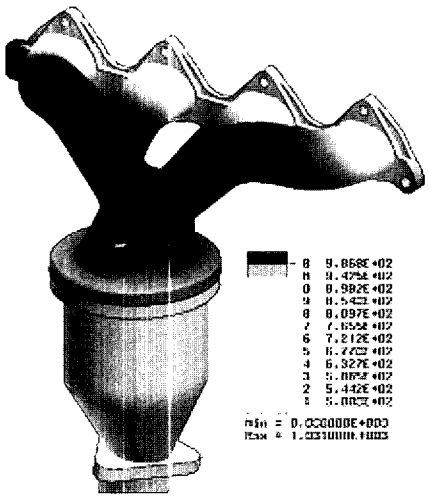

Figure 8. Temperature field at full load.

Figure 8 presents 3-D temperature distribution at rated rpm and WOT condition such as (B) in Figure 7. The results show that the maximum temperature reached about 760°C. And, the temperature difference between the inner and outer surface is about 12°C.

Where, the lower temperature of the inlet flange results from two reasons; (i) exhaust gas doesnt contact with the flange, and (ii) heat is transferred from inlet flange to the cylinder head, because the cylinder head has lower temperature compared to the exhaust manifold due to the coolant. On the other hand, since all exhaust gas merges at runner junction, its temperature becomes higher than that of any other locations.

3.3. Thermal Stress Analysis

In order to calculate thermal stresses and plastic strains in the exhaust manifold for thermal cyclic load, it is necessary to include steady state or transient heat transfer analysis, temperature dependent elasto-plastic material properties, and proper boundary conditions.

In this study, ABAQUS/Standard Ver. 6.1 was used as solver for the nonlinear elastic and plastic stress analysis in a steady state condition. The analysis was carried out by three steps for the same model of the thermal analysis; first, bolt pretension load was applied at each bolt section (John, 1990), and the thermal stress analysis was performed to simulate the heat up and cool down process of the thermal shock condition.

Figure 9 shows the plastic strain range at critical point of the exhaust manifold for the thermal cycle mode. From the figure, it can be seen that the runner junction has maximum plastic range of 0.454%. The results originate from that the thermal expansion of the runners is restricted by cylinder head and inlet flange.

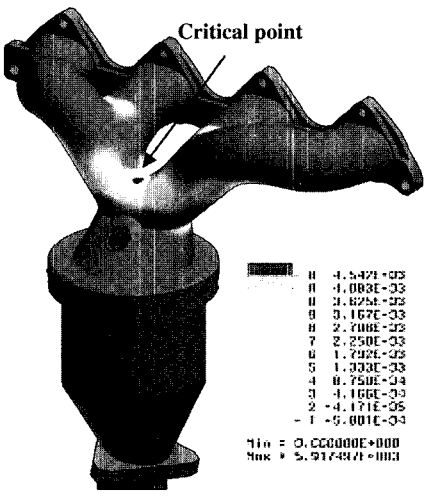

Figure 9. Plastic strain range of the exhaust manifold during thermal cycle mode.

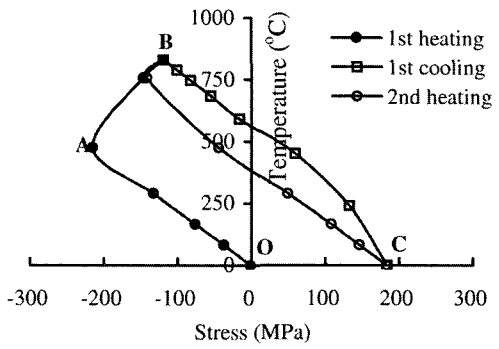

Figure 10. Stress history during thermal cyclic load.

Figure 10 presents the stress history with respect to the temperature for the same location shown in figure 9 (Littler, 1969). As shown in the figure, both the stress and strain between point "O" and point "A" are within the elastic range. Just after that, the manifold presents the initiation of the yield at point "A", and from that point, the stress continues to decrease in spite of the rising temperature until the temperature reaches maximum state at point "B". When the manifold is allowed to cool down, tension stress is created at the same point as the stress moves from point "B" to point "C". As a result, the magnitude of the tensile stress between point "O" and point "C" remains when the manifold is cooled down to the ambient temperature. The later cycles are repeated by the "C-B-C" loop. In this figure, the first yielding point occurs when the temperature reaches nearly 500°C.

3.4. Prediction of the Thermal Fatigue Life

Most failures of the exhaust manifold during the thermal shock are originated by the thermal fatigue due to the compressive strain that occur at high temperature regions, and then turns into a smaller plastic strain at cold condition. Therefore in this study, the plastic strain range in actual exhaust manifold is used as the crack initiation criteria.

The stress-strain response at the crack location can also be plotted as shown in Figure 11. The fatigue failures of exhaust manifold generally occur by the following process.

(1) Compressive plastic deformations are occurred during heating process, since the thermal expansion of the manifold is restricted by the cylinder head and inlet flange.
(2) Tensile stresses are generated during the cooling process.
(3) The cyclic repetition of steps (1) and (2) results in a thermal surface cracks. The initiated crack point then progressively propagates through the thickness and finally failed.

A large strain ε_i developed due to the first compressive strain and then presented some plastic strain range that is stabilized cyclically. As ε_i was generated only by the temperature rise in the first cycle, it has minor effect in developing a thermal fatigue crack. And, although creep may have occurred at an elevated temperature, its effect on the thermal fatigue life is relatively small because at that moment, the exhaust manifold remains in the state of compressive strain. It is therefore concluded that the fatigue failure be dominated mainly by plastic strain range $\Delta\varepsilon_p$.

In order to apply the Coffin-Manson equation for the prediction of the low cycle thermal fatigue of the exhaust manifold, we obtained stress-strain hysteresis loop during thermal load (Manson, 1996).

The curve of number of cycles to failure is plotted as a function of plastic strain range $\Delta\varepsilon_p$. The relationship between plastic strain range and number of cycle to failure shows linear in log-log coordinates as in equation (4).

$$\Delta\varepsilon p = M(2N_f)^z \tag{4}$$

where, M and z are the material constant.

The bench test specification is defined to maintain over 600 cycles for the HMC (Hyundai Motor Company) thermal shock mode. Figure 12 is the modified relationship of the

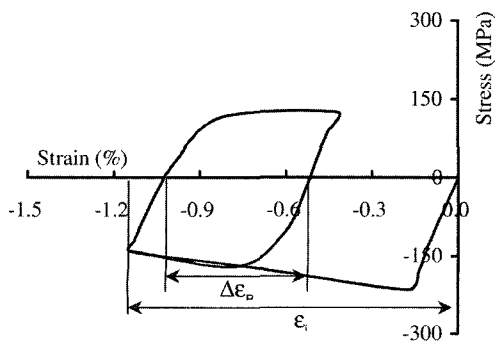

Figure 11. Stress-strain hysteresis loop of a critical point.

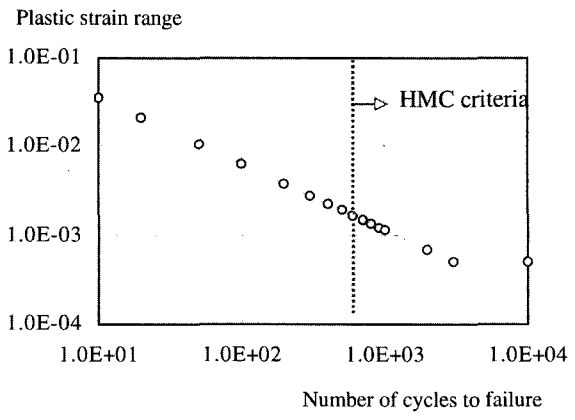

Figure 12. Plastic strain range vs. No. of cycles to failure.

Table 3. Analysis and test result for exhaust manifolds.

Manifold type		$\Delta\varepsilon_P$ (%)	Predicted life (cycle)	Test result (thermal shock)
ENGINE "A"	(1)	0.454	200	Fail
	(2)	0.189	640	Pass
ENGINE "B"	(3)	0.151	440	Fail
	(4)	0.086	920	None
ENGINE "C"	(5)	0.249	240	Fail
	(6)	0.118	650	Pass

analysis results based on the empirical fatigue data.

Table 3 shows the analysis and test results for HMC exhaust manifolds. Comparison of the results between analysis and bench test shows a good agreement in both the temperature history and the crack initiation.

From the results, it is believed that less than 0.180 (%) maximum plastic strain range based on used boundary conditions during the stabilized thermal cycle indicates a safe design (> 600 cycles) for a cast iron exhaust manifold.

4. CONCLUSIONS

The following results were obtained by applying thermal stress analysis procedure to the hot end exhaust system.

(1) Temperature distribution of the exhaust manifold was calculated by CHT analysis. As expected, the collector zones of the runners are very hot, reaching a maximum metal temperature value of 760°C.

(2) By applying the calculated temperature distribution and boundary condition to the finite element model, thermal stress and deformation were calculated. As a result, the maximum plastic strain range of 0.454% was found in a critical location of the runner junction, which corresponds to the 200 cycles of the HMC bench test specification.

(3) Crack initiation criteria for the exhaust manifold was developed using the stress-strain hysteresis loop from the thermal analysis method. It can be concluded that from the internal database of the analysis and test results, the plastic strain range less than 0.180% during the stabilized thermal cycle gives a safe design (> 600 cycles) for the cast iron exhaust manifold. The life prediction technique presented here correlates well with the results obtained from actual engine endurance tests, and is now practically applied in early design stage of the exhaust manifold.

Furthermore, we will extend the analysis method to consider the effects of the strain rate and hold time on the low cycle fatigue behavior of the exhaust manifold. And, it also be included the service vibration load. They are important variables in thermal fatigue and have to be considered in a future study.

REFERENCES

John, H. B. (1990). *An Introduction to the Design and Behavior of Bolted Joints*. M. Dekker, New York and Basel.

Kawano, H., Inoue, S., Iwata, M., Yamaguchi, T., Yanagisawa, H. and Fukumori, E. (1991). Improvement in the thermal elasto-plastic FEM model applied to exhaust manifold. *SAE Paper No.* 911771, 1–11.

Lederer, G., Charkaluk, E., Verger, L. and Constantinescu, A. (2000). Numerical lifetime assessment of engine parts submitted to thermomechanical fatigue. Application to Exhaust Manifold Design, *SAE Paper No.* 2000-01-0789, 1–7.

Littler, D. J. (1969). *Thermal Stresses and Thermal Fatigue*. Buttrerworths. London.

Manson, S. S. (1996). *Thermal Stress and Low-Cycle Fatigue*. McGraw-Hill. New York.

Noguchi, T., Yasuki, T., Nakakubo T. and Atsumi, T. (1985). Thermal stress and deformation analysis of exhaust manifold of internal-combustion engine. *The Society of Automotive Engineers of Japan, Riview*, 34–39.

Watanabe, Y., Shiratani, K., Iwanaga, S. and Nishino, K. (1999). Thermal fatigue life prediction for stainless steel exhaust manifold. *SAE Paper No.* 980841, 1–6.